Volume 305, number 3, 249–253 FEBS 11256 July 1992

Solubilization steps of dark-adapted purple membrane by Triton X-100

A spectroscopic study

Olivier Meyer, Michel Ollivon and Marie-Thérèse Paternostre

Equipe Physico-Chimie des Systèmes Polyphasés, CNRS URA 1218, Université Paris-Sud, 5 rue J.B Clément, 92296 Châtenay-Malabry Cedex, France

Received 4 May 1992; revised version received 22 May 1992

Ultraviolet-visible spectroscopy has been used to follow the solubilization of the dark-adapted purple membrane of *Halobacterium halobium* by Triton X-100. Turbidity of purple membrane fragments and absorbance of bacteriorhodopsin variations during continuous addition of detergent give solubilization profiles exhibiting several break points corresponding to different equilibrium stages of the solubilization process. The present method allows the determination of the detergent to protein + lipid ratio in mixed aggregates at the corresponding break points. It was concluded that, when performed systematically, this technique is a very convenient and powerful tool for the quantitative study of biomembrane-to-micelle transition.

Purple membrane; Bacteriorhodopsin; Triton X-100; Solubilization; Turbidity; Absorbance

1. INTRODUCTION

The knowledge of structural and functional molecular characteristics of integral membrane proteins often requires their purification from native biomembranes, either to reconstitute them into liposomes, or for further studies, including the delicate crystallization process. Before any purification step, the membrane proteins must be solubilized by the use of detergents. An optimal strategy of reconstitution of bacteriorhodopsin (BR), the single protein in the purple membrane (PM) of *Halobacterium halobium*, into large unilamellar vesicles of phosphatidylcholine, has been developed [1]. This strategy consists of rapid detergent removal from solutions containing solubilized BR and lipid–detergent mixtures. Apart from the development of this new strategy, these studies have permitted the determination of distinct optimal conditions of reconstitution depending on the nature of the detergent used. When the non-ionic detergent, Triton X-100 (TX100), is used the solubilized BR needs a certain proportion of detergent–lipid mixed micelles to insert the liposomes bilayer. As far as other membrane proteins are concerned, it was shown [2,3] that the optimal conditions for reconstitution remained identical, indicating that detergent behavior is similar whatever the protein chosen. However, the supramolecular mechanism involved in such reconstitutions has not yet been elucidated.

The thermodynamic reversibility of solubilization and reconstitution processes is nowadays well accepted, both in the case of pure lipid membranes and native biomembranes containing proteins. Detailed knowledge of these processes may help in monitoring the formation of well-defined models of native membranes. Because of its spectroscopic characteristics, easy purification and well-known structure, PM appears to be a good candidate for solubilization studies. Its chromoprotein is organized in a two-dimensional hexagonal lattice of oriented trimers that are surrounded by about 30 lipid molecules per trimer [4,5]. The polypeptide chain forms 7 α-helix segments spanning the membrane. Like visual pigments, BR contains one retinal chromophore bound to Lys-216 as a protonated Schiff-base.

Depending on light exposition, PM may exist either in the light- or dark-adapted form, with a wavelength of the absorbance maxima (λmax) at 570 and 560 nm, respectively. This wavelength shift is related to the proportion of BR retinal isomers within each PM form. Light-adapted PM contains only *all-trans* retinal as the BR prosthetic group, while the dark-adapted form contains a mixture of *all-trans* and *13-cis* isomers [6]. Treatment with TX100 dissociates PM into monomers of BR, shifts the absorption maximum towards lower wavelengths and also decreases the molar absorbance [7]. In the case of dark-adapted PM this blue shift has been

Abbreviations: PM, purple membrane; BR, bacteriorhodopsin; TX100, Triton X-100; LIP, lipid; OD, optical density; R_{eff}, effective TX100 to PM components ratio at break points; HEPES, *N*-(2-hydroxyethyl)-piperazine-*N'*-2-ethanesulfonic acid.

Correspondence address: M.-T. Paternostre, Equipe Physico-Chimie des Systèmes Polyphasés, CNRS URA 1218, Université Paris-Sud, 5 rue J.B Clément, 92296 Châtenay-Malabry Cedex, France. Fax: (33) (1) 46 83 53 12.

interpreted as being due only to chromoproteic environment changes. An additional cause of this shift, however, could be the isomerization of *all-trans* into *13-cis* retinal configuration in the case of the light-adapted form [8,9].

TX100 is one of the rare detergents that can reversibly solubilize PM without significantly affecting BR functional properties. In this study, the controlled solubilization of PM by TX100 was monitored periodically by fast recording of UV-visible spectra. Turbidity variations provided information on the kinds of supramolecular assembly, while absorbance spectrum evolution reported on the molecular BR environment. Several new steps were evidenced during solubilization and the corresponding detergent to protein, or detergent to protein + endogenous lipid ratios in the aggregates were deduced from the measurements.

2. MATERIALS AND METHODS

Purple membrane (19 mg BR/ml) was isolated from *Halobacterium halobium* (strain S9), according to the method of Oesterhelt and Stoeckenius [10] and was a gift from Dr. J.L. Rigaud. Triton X-100 was purchased from Sigma. The buffer solution used for PM and TX100 dilutions and solubilization experiments was 10 mM HEPES (Sigma), 145 mM NaCl (pH 7.4). The optical density (OD) spectra were recorded with a double beam spectrophotometer (Lambda 2, Perkin Elmer) monitored by an IBM-PC computer (PCSS program).

Each sample of PM was sonicated at 4°C for 5 s using a Vibracell Sonics Sonifier (0.5" probe, 10% of full scale power) to homogenize the membrane fragments. The sonicated suspension was then illuminated with a 150 W lamp at 4°C through an anti-caloric filter made of a water-circulating glass jacket (1 cm thick) to get the light-adapted form of the BR. A quartz cuvette containing 1.4 ml of the above-treated PM suspension was then placed in the spectrophotometer at 25°C and the suspension continuously stirred during all the experiments.

The absorbance spectra were measured from 400 to 700 nm with a 1 nm step and recorded every 5 min over 3 h before any detergent addition, in order to allow the PM to return to its dark-adapted form (Fig. 2).

The TX100 solution was continuously added at a constant rate to each PM suspension through a thin tube connected to a glass precision syringe (Hamilton), which was pushed by a syringe pump (Perfuser VI, Braun). The TX100 concentrations in the syringe were adapted to those of the initial PM concentrations to obtain comparable time-courses for solubilizations. These latter were monitored overnight for 12 h and OD spectra were recorded under the same conditions as used for the light-to-dark adaptation phase. All the spectra, taken at constant time intervals, were stored. These data were then analysed using appropriate software in order to deduce the evolutions of OD at both 700 and 560 nm (OD_{700} and OD_{560}) and of the λmax during solubilization. The latter was determined for each spectrum by quadratic regression analysis in the 530–700 nm range.

Since at low detergent concentrations there was some lack of accuracy in λmax determinations, due to the poor signal to noise ratios, all spectra were smoothed using the Savitzky-Golay method [11]. TX100 concentrations values at break points were determined graphically from OD_{560}, OD_{700} and λmax solubilization profiles, as previously described using tangent intersections [12].

3. RESULTS AND DISCUSSION

OD spectra of both light- and dark-adapted forms of a 0.9 mg BR/ml PM suspension are shown in Fig. 1. They correspond to the first and last spectrum recorded during the light-to-dark adaptation phase, respectively. The OD spectrum of the PM results from two contributions: the turbidity due to the light scattering from membrane fragments, and the absorption of retinal molecule bound to the protein. The absorption spectrum of the dark-adapted PM presents a blue shift, compared to the light-adapted PM, and a slight decrease of the maximal OD intensity related to a decrease of the molar extinction coefficient, as shown previously [7]. The evolution of λmax during the light–dark adaptation phase is shown in Fig. 2. λmax determined for the light- and dark-adapted forms of the protein (573 and 565 nm, respectively) are a little higher than those expected for the two forms according to the literature. This could be linked to the slit widths used in our measurements. Furthermore, in the conditions used in the spectrophotometer, after 3 h, the dark adaptation of the BR is not complete since a slight but continuous decrease is still recorded.

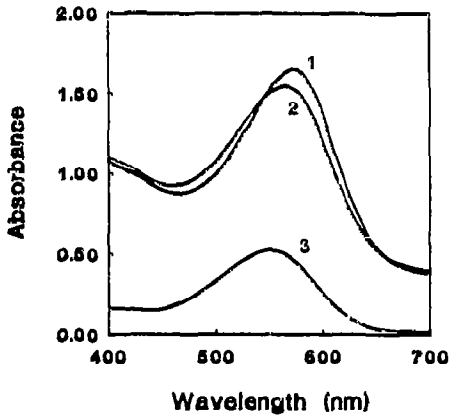

Fig. 1. Effects of light–dark conditions and Triton X-100 addition on the visible absorption band of purple membrane (0.9 mg BR/ml). OD spectrum of light-adapted PM (1), dark-adapted PM (2) and dark-adapted solubilized BR (3).

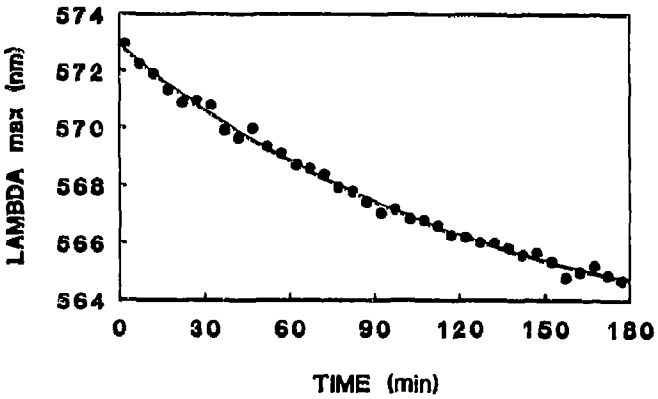

Fig. 2. Kinetics of PM light–dark adaptation. λmax (nm) is plotted as a function of time.

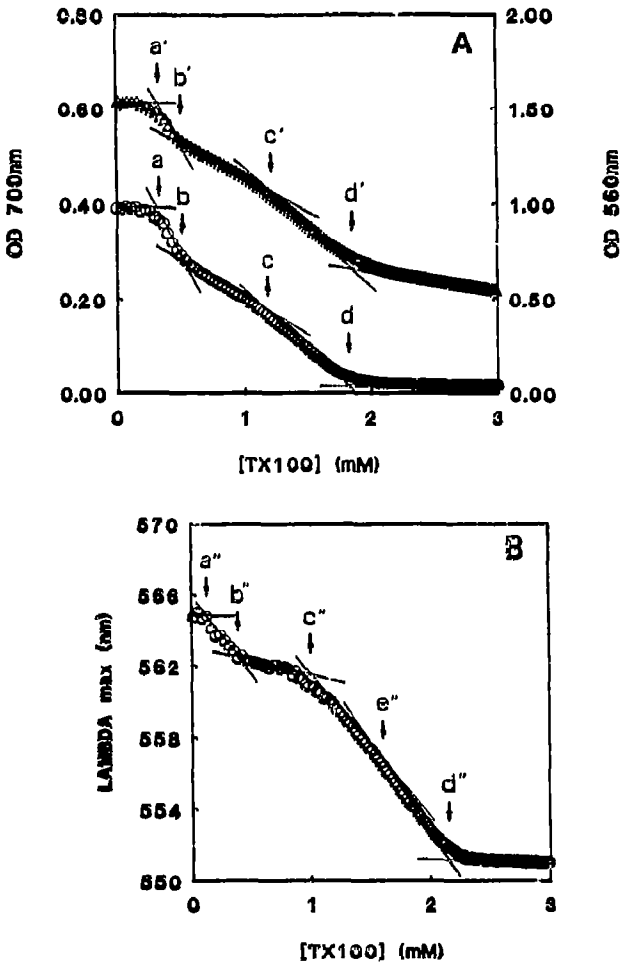

Fig. 3. Solubilization of dark-adapted PM by Triton X-100. (A) OD_{700} (○), OD_{560} (△) and (B) λmax variations of dark-adapted PM (0.9 mg BR/ml) during the continuous addition (0.011 mM/min) of Triton X-100 (7.7 mM).

At the end of solubilization of the dark-adapted form (spectrum 3, Fig. 1), disappearance of turbidity and a blue shift of the absorption band were observed, as previously reported [8]. The changes of both OD_{560} and OD_{700} and λmax vs. TX100 concentration are plotted in Fig. 3A and B, respectively. Like the spectra shown in Fig. 1 these profiles were obtained from the same PM sample (0.9 mg BR/ml). The profiles in Fig. 3A show four break points (denoted a,b,c,d). The corresponding detergent concentrations are similar for both curves, except for d', which is significantly shifted towards higher detergent concentrations. The λmax variations exhibit very similar profiles to those obtained from optical density plots (Fig. 3B), except that one supplementary break point, designated e" is also observed.

Fig. 4A shows the relationship between suspension turbidity and the total detergent concentration for different initial PM concentrations. Increasing the PM concentration shifts OD curves towards higher [TX100]. In Fig. 4B the detergent concentrations needed to reach the different break points are plotted vs. PM concentration. As the [PM] may be expressed either by the BR content (in mg/ml) or by the sum of BR and lipid ([BR]+[LIP]) content (in mM) of the sample, assuming lipid/BR=10 (mol/mol) in the native PM, both scales are expressed in the figure. The same analysis has been undertaken to relate [TX100] to BR content using λmax dependence on [TX100] (Fig. 4C). In all cases, interestingly, for each break point, linear relationships are observed between [TX100] and [BR] (or [BR]+[lipid]). The slopes deduced from linear regression analysis correspond to the [detergent]/([protein]+[lipid]) in mixed aggregates found at the corresponding break points. By analogy with solubilization of phosphatidylcholine vesicles by detergents [13,14] each break point seems to correspond to limit steady-state conditions between two steps occuring in each solubilization process. The values of the effective ratios (R_{eff}) determined from each linear relation slope are reported in Table 1.

A comparison of the four slopes calculated (Fig. 4B) from turbidity measurements during solubilization of dark-adapted PM at different concentrations to the five deduced from the variation of their λmax (Fig. 4C) shows that both break points, b and c, occur at the same [TX100] as break points noted b" and c" respectively, indicating that the same transition is seen from turbidity and λmax curves. Therefore, at these break points, changes of aggregate size and protein microenvironment appear simultaneously. It should be noted that good agreement between the two sets of linear regression plots of Fig. 4 (B and C) was obtained. On the other hand, it was not possible to establish similar relations

Table 1

Effective ratios at break points from OD_{700}, OD_{560} and λmax

	Break points				
	a / a' / a'	b / b' / b'	c / c' / c'	e'	d / d' / d'
TX100/BR+LIP (mol/mol)	0.94/0.98/0.44	1.42/1.39/1.49	3.69/3.68/3.55	5.90	6.62/7.31/8.25
TX100/BR[a] (mM/mg · ml^{-1})	0.38/0.42/0.19	0.61/0.59/0.63	1.57/1.56/1.51	2.53	2.80/3.09/3.48

[a]The BR concentrations in mixed aggregates are expressed in mg/ml as usually used in the literature

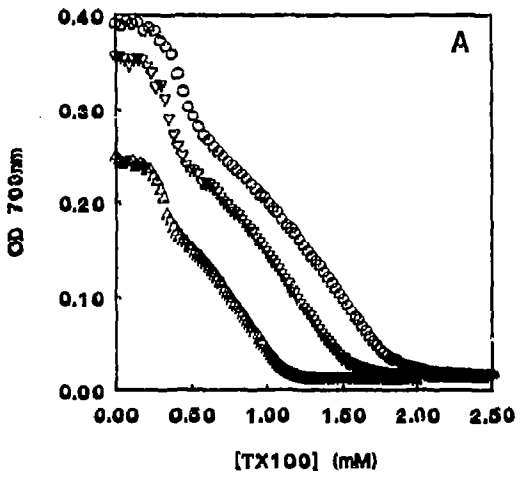

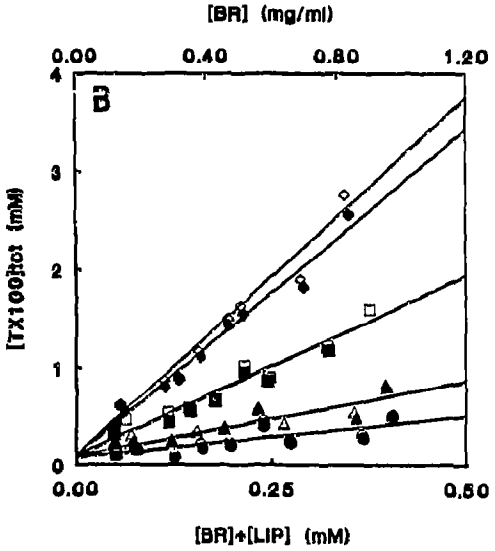

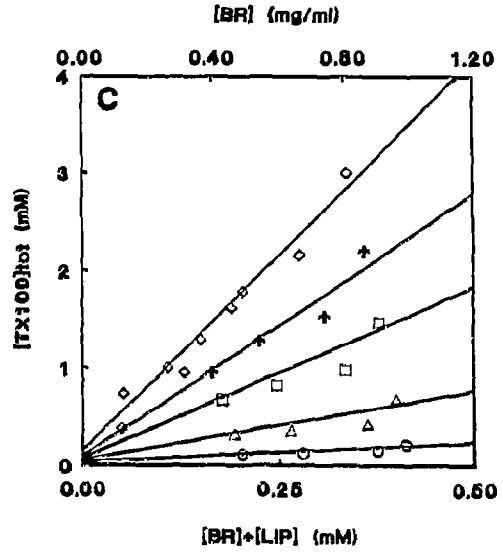

for break points a and a" or d and d", points a" being observed at lower TX100 concentrations than those measured for break points a. This observation suggests that when TX100 is continuously added to PM fragments, the change in BR environment caused by this addition takes place *before* any decrease of the membrane fragment size. This can be explained by the fact that even at very low [TX100], detergent monomers partition between aqueous and membrane phases, the interaction being detected first in the BR environment.

The solubilization of PM by TX100 appears to be a step by step de-lipidation of the PM causing membrane fragments to break up from point a to d, above which all PM components are kept in micellar structures.

Break points noted b(b") and c(c") cannot yet be attributed to any precise events, but it is reasonable to think that they could be related to the destructuration of the two-dimensional lattice and the monomerisation of BR steps, respectively. The break point denoted e" represents an equilibrium state where a change of environment occurs whithout any further modification of the aggregate size. It is known that PM lipids are solubilized by TX100 more easily than protein, so that hardly any protein is solubilized at detergent concentrations at which about 75% of lipids are kept in detergent- mixed micelles [9]. Thus, this step may correspond to a change in the BR solubilization process which does not affect the progressive average size decrease of the mixed protein–lipid aggregates, where TX100 starts to solubilize BR rather than further solubilizing PM lipids.

Finally, the values of the [TX100] measured at break point d" is significatively higher than those required to reach break point d and even d'. Thus, the BR environment is still being modified when no further decrease of aggregate size can be detected. From break point d, either there are further changes in the unique mixed ternary micelles (protein–lipid–detergent), or the solubilized PM samples contain at least two mixed micelles populations, one composed of detergent–lipid micelles, and another composed of binary (detergent–protein) and/or ternary (detergent–protein–lipid) micelles. In both cases, within the TX100 concentration range between break points d and d", the detergent molecules would probably be more and more able to attain hydrophobic regions of BR and better surround each protein helix, causing further modifications of retinal environment. Either increasing or decreasing protein–lipid in-

←

Fig. 4. Solubilization and TX100–PM phase diagram. (A) OD_{700} is plotted vs. [TX100] at several [PM]: (○) 0.9 mg BR/ml; (▽) 0.68 mg BR/ml and (△) 0.49 mg BR/ml. (B) $[TX100]_{tot}$ is shown as a function of [BR] and [BR]+[LIP] at break points a (circles), b (triangles), c (squares) and d (diamonds). Filled symbols are from turbidity and open symbols are from OD_{560} measurements taken during dark-adapted PM solubilization. (C) The same relations are plotted from λmax measurements at break points a" (circles), b" (triangles), c" (squares), d" (diamonds) and e" (crosses).

teractions, or a combination of both, could easily explain these last spectroscopic data.

In Fig. 3A, the OD_{560} profile exhibits a quasi-linear decrease of the BR molecular extinction coefficient beyond point d', which is not observed at 700 nm, indicating a PM bleaching, as already described by Gonzáles-Mañas et al. [9] for the light- adapted PM and interpreted in terms of TX100-catalysed hydrolysis of the Schiff-base linking BR apoprotein to retinaldehyde. This phenomenon is observed here in the case of the BR dark-adapted state. It should be noted that although this process is only observed beyond break point d', it is likely that it starts before, i.e as soon as TX100 molecules directly interact with retinal.

4. CONCLUSIONS

The relationship between detergent and BR and lipid content is linear, confirming the analogy between phospholipidic vesicles and biomembrane solubilization by detergents. These linear dependencies can be described by the equation

$$[TX100]_{tot}=[TX100]_{free} + R_{eff}([BR]+[LIP])$$

where $[TX100]_{tot}$ represents the total concentration of TX100 added to the PM solutions, $[TX100]_{free}$ the monomeric detergent concentration in equilibrium with mixed aggregates and R_{eff} the effective $[TX100]_{ag}$ (i.e the [TX100] present in those aggregates) to [BR]+[LIP] ratio.

Because of the imprecise determination of initial PM concentrations and, furthermore, because of the rather low critical micellar concentration of TX100 (0.24 mM), the $[TX100]_{free}$ values estimated from the intercept of the respective lines at zero [BR]+[LIP] are not significant. Nevertheless, the ratio values calculated from the slope of each straight line are hardly affected by these factors and give good and coherent data.

From this work, it is possible to estimate the quantity of detergent in direct interaction with protein if the concentration of detergent in interaction with lipids is known. Studies presently in progress in our laboratory, concerning the solubilization of small sonicated vesicles composed of different lipid mixtures of phosphatidylcholine, phosphatidylethanolamine, phosphatidylserine and sphingomyelin by TX100, show that, at the end of solubilization, the detergent to lipid ratio ranges between 2.5 and 3 whatever the lipidic vesicle composition [15]. If this were the case for PM endogenous lipids, which are all bicatenary lipids like those studied, one can subtract from detergent concentration in interaction with both PM lipids and BR the quantity of detergent necessary to solubilize the lipids alone. This new calculated TX100 to BR ratio ranges between 60 and 68 (mol/mol). This estimation indicates that at the end of the solubilization process (point d"), the solutions contain, at least, mixed micelles in which about 64 molecules of TX100 interact with one BR monomer. This result suggests that each BR helix would be surrounded by about 9 detergent molecules, implying at least some hydrophobic interactions.

We report here a very powerful spectroscopic method which gives access to molecular aggregate composition during solubilization of biomembranes by detergents. Such a study is very useful for characterizing the membrane–micelle transition intermediates, and thus, determining the molecular mechanisms involved in the solubilization of membrane proteins. The solubilization of other integral membrane proteins can be studied as described here, provided that they exhibit some specific biophysical characteristics. The present work provides a rationale for future structural analysis of mixed aggregates which coexist at each equilibrium state in the solubilization process. Additionally, it may be of interest for membrane protein crystallographs to be able to determine, using this method, the detergent to protein ratio necessary to obtain optimal conditions in crystal growth and quality.

Acknowledgements: We thank G. Barrat for correcting the English.

REFERENCES

[1] Rigaud, J.L., Paternostre, M.T. and Bluzat, A. (1988) Biochemistry 27, 2677–2688.
[2] Richard, P., Rigaud, J.L. and Gräber, P. (1990) Eur. J. Biochem. 193, 921–925.
[3] Lévy, D., Bluzat, A., Seigneuret, M. and Rigaud, J.L. (1990) Biochim. Biophys. Acta 1025, 179–190.
[4] Oesterhelt, D. and Stoeckenius, W. (1971) Nature (New Biol.) 233, 149–152.
[5] Blaurock, A.E. and Stoeckenius, W. (1971) Nature (New Biol.) 233, 152–154.
[6] Scherrer, P., Mathew, M.K., Sperling, W. and Stoeckenius, W. (1989) Biochemistry 28, 829–834.
[7] Casadio, R., Gutowitz, P., Mowery, P., Taylor, M. and Stoeckenius, W. (1980) Biochim. Biophys. Acta 590, 13–23.
[8] Gonzáles-Mañas, J.M., Montoya, G., Rodrigez- Fernández, C. (1990) Biochim. Biophys. Acta 1019, 167– 169.
[9] Gonzáles-Mañas, J.M., Virto, M.D., Gurtubay, J.I.G. and Goni, F.M. (1990) Eur. J. Biochem. 188, 673–678.
[10] Oesterhelt, D. and Stoeckenius, W. (1974) Methods Enzymol. 31, 667–678.
[11] Savitzky, A. and Golay, M.J.E. (1964) Anal. Chem. 36, 1627–1639.
[12] Lesieur, S., Grabielle-Madelmont, C., Paternostre, M.T., Handjani-Vila, R.M and Ollivon, M. (1990) Chem. Phys. Lipids 56, 109–121.
[13] Ollivon, M. Eidelman, O. Blumenthal, R. and Walter, A. (1988) Biochemistry 27, 1695–1703.
[14] Paternostre, M.T., Roux, M. and Rigaud, J.L. (1988) Biochemistry 27, 2677–2688.
[15] Champagne, N., Ollivon, M. and Paternostre, M.T. (in preparation).